Combined wave – iceberg loading on offshore structures

Ricardo Foschi, Michael Isaacson, Norman Allyn, and Steven Yee

Abstract: The Canadian Standards Association has developed and published a code for the design and construction of fixed offshore structures. This code has been subjected to a comprehensive verification process which has identified several issues warranting further study. One of these relates to the combined effects of wave and iceberg collision loading. At present, this combination is treated by the use of a load combination factor specified in the Code. The present paper describes a recent study which was undertaken to determine the appropriateness of the recommended value of the load combination factor. The study involves a numerical analysis in which loads due to waves alone, an iceberg alone, and an iceberg and waves in combination have been calculated for a range of iceberg and wave parameters. These results have been applied to a first-order reliability analysis in order to study the force levels corresponding to an annual probability of 10^{-4} or to the onset of global sliding with an annual probability of 10^{-4}. The paper thereby makes recommendations for load combination factors applicable to combined wave–iceberg loading.

Key words: hydrodynamics, icebergs, ocean engineering, offshore structures, wave forces, waves.

Résumé : L'Association Canadienne de Normalisation a développée et publiée un code de règles de calculs pour la conception et la construction de structures offshore fixes. Ce code a fait l'objet d'un processus de vérification approfondi qui a permit d'identifier plusieurs questions justifiant des études supplémentaires. L'une de ces questions est relative au cas du chargement de collision causé par les effets combinés de la houle et d'icebergs. À l'heure actuelle, cette combinaison est traitée au moyen de l'utilisation d'un facteur de combinaison de charges spécifié par le code. Le présent article décrit une étude récente qui a été entreprise afin de déterminer la convenance de la valeur recommandée pour le facteur de combinaison de charges. L'étude comprend une analyse numérique dans laquelle des chargements dus à la houle seule, à un iceberg seul et à une combinaison des deux ont été calculés pour tout un éventail de paramètres de houle et d'iceberg. Ces résultats ont étés appliqués à une analyse de fiabilité du premier ordre afin d'étudier les niveaux de forces correspondants à une probabilité annuelle de 10^{-4} ou au début du glissement global avec une probabilité de 10^{-4}. L'article fait ainsi des recommandations pour des facteurs de combinaison de charges applicables au cas de chargements combinés houle–iceberg.

Mots clés : hydrodynamique, icebergs, technologie marine, structures offshore, forces de la houle, houles.
[Traduit par la rédaction]

Introduction

The selection of suitable environmental loads and load events is of critical importance in the design of offshore structures intended for operation in extreme environments. Such loads may include those due to wind, waves, earthquakes, ice, and iceberg collisions. The CSA Offshore Structures Code CAN/CSA-S471-92(S471) (Canadian Standards Association 1992), which was finalized in early 1992 and is currently in use, describes the use of such loads in offshore design, and indicates the use of probabilistic methods on which the selection of load events and design loads should be based. The Code has been subjected to a comprehensive verification process, and this has identified several issues which warrant further study. One of these is an assessment of the combined effects of wave and iceberg collision loading. At present, this combination is treated by the use of a load combination factor specified in the Code. The present paper describes a recent study which was undertaken to determine the appropriateness of the current recommendations.

Wave–structure interactions (in the absence of icebergs) has been studied extensively (e.g., Sarpkaya and Isaacson 1981). In the case of large offshore structures, linear diffraction wave theory is generally used to calculate wave loads. This is based on the assumption of potential flow theory, a horizontal seabed, and small amplitude waves. Structures of arbitrary shape are usually treated by a boundary element method in which the submerged surface of the structure is specified in discretized form. Closed-form solutions also exist for a number of reference configurations, the most widely used being the case of a vertical circular cylinder extending from the seabed to the free surface.

Iceberg–structure interactions (in the absence of waves) have also been studied extensively, and an overview of this topic has been given by Cammaert and Muggeridge (1988).

Received August 14, 1995.
Revised manuscript accepted March 13, 1996.

R. Foschi and M. Isaacson. Department of Civil Engineering, The University of British Columbia, Vancouver, BC V6T 1Z4, Canada.
N. Allyn and S. Yee. Westmar Consultants Inc., 400 – 233 W 1st Street, North Vancouver, BC V7M 1B3, Canada.

Written discussion of this paper is welcomed and will be received by the Editor until February 28, 1997 (address inside front cover).

In general, the maximum iceberg load on a structure is obtained by an energy balance in which the initial kinetic energy of the iceberg is equated to the energy dissipated through ice crushing up to the time the iceberg is brought to rest. Topics of particular interest in this regard include the consideration of energy dissipation through structural damage or ductility, and an assessment of the importance of size (area) effects on the ice-crushing pressure.

Wave effects on iceberg motions and the case of waves and an iceberg acting simultaneously on an offshore structure have also been widely studied, although perhaps not to the same extent. Particular aspects which have been considered include wave-induced iceberg motions (e.g., Lever and Sen 1987; Lever et al. 1988), iceberg interactions with semi-submersible rigs (e.g., Lindberg and Andersson 1987; Lever et al. 1990), and iceberg motions near a large structure (e.g., Isaacson, 1987; Isaacson and Dello-Stritto 1987). Isaacson (1987) considered the effect of waves on an iceberg up to the instant of impact with a large structure, and described a numerical model for evaluating iceberg drift motions in order to provide an assessment of wave effects on the iceberg velocity and effective mass at the time of impact.

The present paper describes a numerical analysis in which loads due to waves alone, an iceberg alone, and an iceberg and waves in combination have been calculated for a range of iceberg and wave parameters. These results have been used to develop expressions for wave and iceberg loads which are then used in a probabilistic study of the load event. The probability of failure in global sliding is studied using the first-order reliability method (FORM), with the objective of deriving the load combination that leads to an annual risk of 10^{-4}. As a case study, the paper analyses conditions similar to those of the Hibernia platform to be located in the Grand Banks off the Newfoundland coast. This platform is a gravity-based reinforced concrete structure and will be protected from iceberg impact by a concrete cylindrical wall. In this study, the structure is assumed to be a vertical circular cylinder of radius $a = 58$ m located in a water depth of $d = 80$ m.

Probabilistic framework

Probabilistic analyses have previously been used in offshore engineering problems (e.g., Fuglem et al. 1991; Det Norske Veritas 1988; Maes and Jordaan 1984) and in the calibration of the Canadian code for offshore structures (e.g., Maes 1986). In the present study, however, the probabilistic framework includes the formulation of detailed mechanical and hydrodynamic models for the interaction of waves and icebergs during a collision. Thus, in what follows, a detailed description is given on the approaches used to assess the loads due to waves alone, an iceberg alone, and waves and an iceberg acting in combination.

The estimation of conditional probabilities associated with a load event is conducted using the program RELAN (RELiability ANalysis), developed at the Department of Civil Engineering of The University of British Columbia (Foschi et al. 1990). This program implements standard FORM and SORM algorithms (first- or second-order reliability methods) to calculate the probability that a "performance function" G of the vector of a set of random variables $\mathbf{x}$ is negative. In order to equate this result to an exceedence or failure probability in the present context, the function $G(\mathbf{x})$ is written as follows:

Case (i): To compute exceedence probability of the load level F,

$$[1] \qquad G(\mathbf{x}) = F - F_M(\mathbf{x})R_{n1}$$

Case (ii): To compute probability of global sliding,

$$[2] \qquad G(\mathbf{x}) = W_n R_{n3} \tan(R_{n2}) - F_M(\mathbf{x})R_{n1}$$

where, in both cases, $F_M(\mathbf{x})$ is the maximum force developed on the structure due to waves, or iceberg impact, or waves and iceberg impact in combination, as appropriate, $\mathbf{x}$ denotes a set of specified random variables characterizing the structure, the iceberg, and the wave conditions, and R_{n1} is a random variable associated with model inaccuracy in the calculation of F_M (Bea 1992). For the sliding limit state, W_n is the nominal or mean weight of the structure, R_{n2} is a random variable equal to the sand friction angle, and R_{n3} is a random variable associated with uncertainty in the estimation of the actual weight. In the sliding limit state, probabilities of failure can be obtained for different values of the nominal weight W_n.

In case (*i*) the probability of the event $G < 0$ corresponds to the probability that the maximum load F_M exceeds the load level F. In case (*ii*), the probability of the event $G < 0$ corresponds to the probability that F_M exceeds the sliding capacity. RELAN is a general reliability analysis program which must be supplemented with a specific description of the limit state being analysed. Thus, three specific programs were developed for this study:

- WLOAD: for forces due to waves alone;
- ICELOAD: for forces due to iceberg collisions only;
- ICEWLOAD: for forces due to combination of waves and simultaneous iceberg collision.

Each of these programs can be run under one of four options:

- Option 1: to compute exceedence probability of force level F, assuming a rigid structure;
- Option 2: to compute exceedence probability of force level F, taking into account structural ductility and damage;
- Option 3: to compute probability of sliding, assuming a rigid structure;
- Option 4: to compute probability of sliding, taking into account structural ductility and damage.

In the case of an iceberg impact in the absence of waves, the force exceedence probability is first obtained conditional on the occurrence of an impact. In such a case, the programs allow for the estimation of the corresponding annual risk, denoted p_a, using the hypothesis that the events (i.e., iceberg impacts) follow a Poisson pulse process with a given mean rate of annual occurrence (events per year), denoted μ. Thus, if the conditional exceedence probability of the event is p_e, the annual risk is given as

$$[3] \qquad p_a = 1 - \exp(-\mu p_e)$$

The mean rate of collision events, μ, has recently received some attention (e.g., Fuglem et al. 1996). For the purpose of this work, μ has been assumed to take values ranging from 0.04 to 1.00.

In the case of waves alone, the force exceedence annual risk is directly obtained using annual maxima distributions for the sea state. Therefore, in this case, [3] is not used.

In the case of an iceberg impact in the presence of waves, the force exceedence probability is first obtained conditional on the occurrence of an impact, so that once more [3] is needed to transform this conditional probability into the corresponding annual risk. In this case, the probability distributions for the wave parameters correspond to the sea state which is present at the time of impact, and are based on measured records of wave periods and heights at a specified recording interval τ, taken here as 6 h.

In each of the three cases above, the maximum force F_M developed during the event requires an appropriate mechanics model for its calculation. The following sections describe in turn such calculations for waves alone, an iceberg alone, and waves and an iceberg in combination.

Forces due to waves alone

An analysis is first carried out for wave loads in the absence of icebergs. A simple representation of the maximum annual distribution of wave conditions is initially required, and a single parameter, the peak period T, is used here. The maximum annual wave period is assumed to obey an extreme type I annual probability distribution (e.g., Sarpkaya and Isaacson 1981), such that $T = 18$ s corresponds to a cumulative probability $p = 0.99$ (return period $T_R = 100$ years); and $T = 15$ s to $p = 0.05$ ($T_R = 1.05$ years). Thus,

$$[4] \quad p(T) = \exp[-\exp(-1.8991(T - 15.5777))]$$

where T is in seconds. The significant wave height H_s (m) can be estimated from a formula which has been found to be suitable for conditions in Canadian Atlantic waters (Neu 1982):

$$[5] \quad H_s = 0.0509T^2$$

From [4], this corresponds to significant heights of 16.49 m and 11.45 m for probability levels $p = 0.99$ and $p = 0.05$, respectively.

The loads for regular waves may be obtained from an analysis based on linear diffraction theory. Results are obtained using a computer program WELSAS, which is based on three-dimensional linear diffraction theory using a boundary element method (e.g., Sarpkaya and Isaacson 1981). The program involves a discretization of the submerged structure surface into quadrilateral elements, and employs a suitable Green's function. The pressure distribution on the structure's surface is integrated to obtain the total force. Although a closed-form solution is available for a vertical circular cylinder (e.g., Sarpkaya and Isaacson 1981), this solution is simply used to verify the results of WELSAS for the case of waves alone, since the computer model is needed for the subsequent case of combined wave–iceberg loading. For regular waves of height H and period T, the force on the structure varies sinusoidally with period T, and thus is expressed as $F\cos(\omega t)$, where $\omega = 2\pi/T$ and F is the force amplitude. F is proportional to the wave height, so that results need only be obtained for waves of unit height. Since the wave forces are ultimately required for application in a probabilistic model, a simple expression has been fitted to numerical results obtained for wave periods T ranging from 10 to 20 s. The results correspond to a water depth of 80 m, a water density of 1025 kg/m^3, and a structure of radius 58 m. Thus, for the case of regular waves alone, the maximum force $F_M = F$ on the structure is thereby obtained in the form:

$$[6] \quad F = H[-136.807 + 22.546T - 0.593T^2]$$

where F is in MN and T and H are, again, the wave period (s) and the wave height (m) respectively. For a wave period T of 18 s, with 0.01 annual exceedence probability, the significant wave height H_s is 16.49 m and the corresponding force is 1268 MN.

The loads due to random waves may be obtained as an extension of the case of regular waves. However, the wave height H is now random and obeys a Rayleigh distribution, the cumulative distribution of which is

$$[7] \quad p(H) = R_{n7} = 1 - \exp\left[-2\left(\frac{H}{H_s}\right)^2\right] \quad \text{for } H \geq 0$$

where R_{n7} is a random variable uniformly distributed between 0 and 1. For a particular pair of random wave height and period values, H and T, the corresponding force may be obtained from [6].

Force due to iceberg collision alone

The force developed during an iceberg collision will vary during the process of ice crushing against the structure, since the area of contact is continuously changing and the crushing pressure exhibits a notable size effect (the greater the contact area, the lower the required pressure). The force is also influenced by the damage deformation of the structure, which may have been designed to allow for local damage when the force exceeds a certain level. Here, local damage is associated with the deformation or collapse of the structure in the neighbourhood of the contact point with the iceberg. Of course it is quite difficult to derive relationships between applied pressure and structural damage during a situation of progressive collapse. The software developed for this study can consider the energy dissipation through local structural collapse, on the basis of an assumed relationship between applied force and the additional iceberg penetration due to structural damage.

The necessary background of ice mechanics and risks to offshore structures have been amply discussed elsewhere (Sanderson 1988). The present study applies such basic concepts to the particular example under consideration here, similar to that of the Hibernia platform, and extends the formulation to take account of iceberg penetration due to local structural damage. The size effect in ice crushing pressure is also considered.

Iceberg shape and size

Of course it is very difficult to represent accurately the three-dimensional shape of a realistic iceberg by a mathematical equation. The approach adopted here follows that of Det Norske Veritas (1988), in which the iceberg is assumed to be circular in plan and ellipsoidal in elevation (Fig. 1), with

Fig. 1. Definition sketch of iceberg–structure geometry.

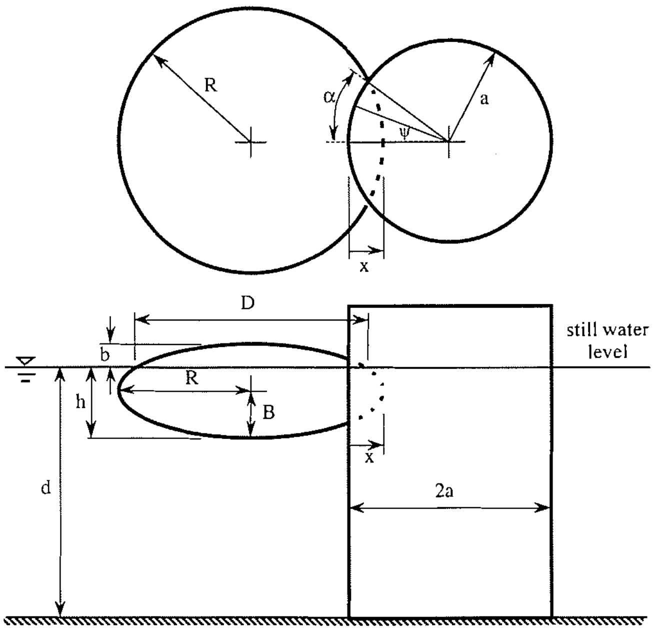

horizontal (major) and vertical (minor) semiaxes R and B respectively. From statistical data for the Grand Banks, all the iceberg dimensions are expressed in terms of a single random variable L (m) which is represented by a Gamma distribution, with a mean value μ_L of 121.60 m and a standard deviation σ_L of 56.70 m. Other characteristic dimensions of the iceberg may be expressed in terms of L. In particular, the horizontal semiaxis R and the iceberg diameter at the waterline, D, are given respectively as

$$[8] \quad R = 0.428L + 1.053L^{0.63}$$

$$[9] \quad D = 0.679L + 1.671L^{0.63}$$

It can be shown that the vertical semiaxis B and the iceberg height above the water, b, are related to the draft h according to

$$[10] \quad B = \frac{h}{1.608}$$

and

$$[11] \quad b = 0.244h$$

respectively.

The iceberg draft h is in turn related to L, except that icebergs capable of colliding must have a draft smaller than the water depth of 80 m. Thus,

$$[12] \quad h = \min \begin{cases} 3.781L^{0.63} \\ d \end{cases}$$

Using the specified Gamma distribution for L, [12] is used to obtain a corresponding distribution of the draft h. Taking account of the truncation at a maximum of 80 m, the data for h have been fitted with a Beta distribution with a minimum of 0 m and a maximum of 80 m, resulting in a mean draft μ_h of 61.35 m with a standard deviation σ_h of 12.38 m.

Ice-crushing pressure

For different penetrations x into the ice, as shown in Fig. 1, it is possible to compute the area of contact as the intersection of the ellipsoid with the cylindrical structure of radius a. From a knowledge of the relationship between ice-crushing pressure and area, the force $F(x)$ may then be obtained by integration, assuming that the pressure is uniformly distributed over the area. The impact is assumed to be head-on, and the contact area is computed accordingly. The possibility of eccentric impact is taken into account through the use of a modification factor, which is subsequently described.

The pressure p required to crush the ice depends on the area of contact A. It is assumed that the crushing pressure p has a lognormal distribution, with mean μ_p and coefficient of variation V_p:

$$[13] \quad p = \frac{\mu_p}{\sqrt{1 + V_p^2}} \exp\left[R_{n4}\sqrt{\ln(1 + V_p^2)}\right]$$

where R_{n4} has a standard normal distribution (with a mean of 0, and a standard deviation of 1).

In general, the size effect for the mean pressure μ_p can be written in the form:

$$[14] \quad \mu_p = \max \begin{cases} C_1 A^{C_2} \\ p_o \end{cases}$$

Although data on iceberg ice are scarce, the scatter in available data for ice in Arctic conditions (Blanchet 1990) is reasonably well represented with the following values of the parameters in [14]:

$$V_p = 0.50$$

$$C_1 = 9.0 \text{ MPa}$$

$$C_2 = -0.5$$

$$p_o = 2.0 \text{ MPa}$$

with A in m^2. The value p_o is a lower bound for μ_p. Due to uncertainty in ice-crushing pressure for large areas A, it may be more appropriate to represent p_o by a suitable probability distribution. Instead, in the present study, p_o is taken as a constant. It should be noted that the lower bound p_o = 2 MPa is reached at a contact area of about 20 m^2, which is probably very quickly exceeded during a collision. The value of p_o is not well defined from available data, and since it is expected to have marked influence on the loads developed during the collision, three specific values of p_o are studied: 2, 4, and 6 MPa in turn.

Force–penetration relationship

For a given penetration x due to ice crushing (see Fig. 1), the force $F(x)$ acting on the structure can be calculated from an integration of the crushing pressure p over the area of contact $A(x)$:

$$[15] \quad A(x) = 2a \int_0^{\alpha} s(x, \psi)\, d\psi$$

$$[16] \quad F(x) = 2ap(x) \int_0^{\alpha} s(x, \psi) \cos\psi\, d\psi$$

Fig. 2. Iceberg collision force as a function of penetration for two iceberg sizes.

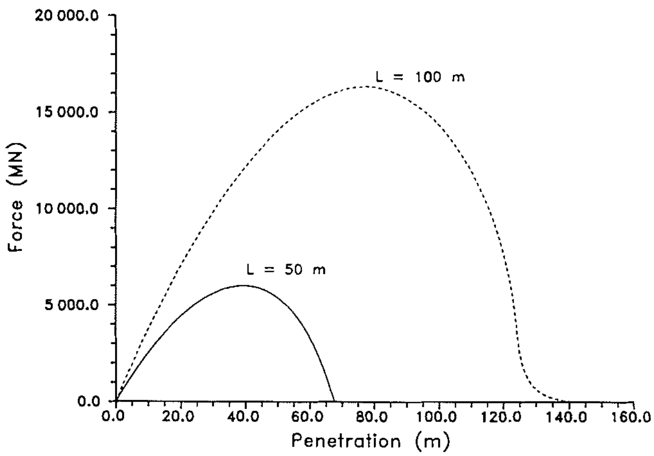

where the angles α and ψ are shown in Fig. 1, and s is the height of the contact area corresponding to the angle ψ. Figure 2 shows two typical force–penetration relationships, for $L = 50$ m and $L = 100$ m. For a relatively small iceberg with $R < a$, and assuming sufficient kinetic energy, the iceberg could eventually disintegrate against the structure; for a relatively large iceberg with $R > a$, the structure would split the iceberg into two. However, these two situations represent extreme events. In general, it is found that in the cases of interest, the iceberg will be stopped after a few metres of penetration, near the beginning of the curves like those in Fig. 2. In fact, the force–penetration relationship has an infinite slope at zero penetration. However, the slope becomes finite very quickly and this initial effect cannot be distinguished when the complete curve is plotted as shown in Fig. 2. The relationship may thus be linearized for penetrations up to a few metres. In the present case, this linearization is achieved by replacing the curve with a straight line fit to results for penetrations up to 2 m.

Impact velocity

An iceberg will impact the structure with a velocity V which influences the magnitude of the maximum iceberg force on the structure. The impact velocity V is generally influenced by the prevailing current, wind, and waves. For simplicity, the impact velocity V in calm water (iceberg alone, no wind or waves) is taken here to be equal to the current velocity U:

$$[17] \quad V = U$$

This approximation is only needed with respect to the statistical descriptions of V and U, and is reasonably consistent with dynamic models of iceberg drift (e.g., El-Tahan et al. 1986; Isaacson 1988) when applied in the absence of waves and wind. Following data from Det Norske Veritas (1988), the current U is assumed to possess a lognormal distribution, with a mean μ_U of 0.32 m/s and a standard deviation σ_U of 0.27 m/s.

Maximum force

In calm water, the calculation of the maximum force F_M is implemented through consideration of an energy balance. The iceberg will be stopped when its kinetic energy is fully dissipated through ice crushing and structural damage deformation. Thus, this energy balance may be expressed as

$$[18] \quad \frac{1}{2}M(1 + C_m)V^2 = \int_0^{x_c} F(x)\,dx + \int_0^{x_d} F(x)\,dx$$

where the iceberg mass M has been augmented by the added-mass coefficient C_m accounting for hydrodynamic effects. The right-hand side represents the summation of the two cross-hatched areas in Fig. 3. The first term corresponds to the energy dissipated through ice crushing up to a penetration x_c, obtained from the force–penetration relationship. The second term corresponds to the energy dissipated through the local structural damage penetration x_d, and is taken into account only when the force exceeds a minimum force F_o required to produce damage.

The relationship between force and damage penetration has been estimated on the basis of a previous structural analyses of reinforced concrete elements at ultimate load. For the particular ice wall considered here, the results can be represented by a linear relationship up to a damage penetration of 1.5 m, according to

$$[19] \quad F(x) = F_o + 1567 x_d R_{n5} \quad \text{(MN)}$$

with $F_o = 610$ MN. To account for the uncertainty in this estimate, the random variable R_{n5} is introduced, and is assumed to possess a lognormal distribution with a mean of 1 and a standard deviation V_f.

Given the geometry of the iceberg, its impact velocity, and the crushing pressure parameters, [18] can be solved iteratively to obtain the penetrations x_c and (if damage occurs) x_d. Once these are found, the maximum force F_M is obtained from the force–penetration relationship.

Eccentric collisions

The preceding description of the force–penetration relationship and the associated maximum force on the structure is based on the assumption of a head-on collision, whereas in practice an iceberg is likely to impact the structure in an eccentric manner. The influence of eccentric collisions has been considered, for example, by Bass et al. (1985) and Salvalaggio and Rojansky (1986). In order to account for the possibility of eccentric collisions, the maximum force F_M calculated in the manner described is multiplied by an eccentricity reduction factor $K_e \leq 1.0$. Data from Salvalaggio and Rojansky (1986) are utilized to express K_e as

$$[20] \quad K_e = \cos^{0.228}\left(\frac{R_{n6}\pi}{2}\right)$$

where R_{n6} is a random variable with a uniform distribution over the range 0 to 1. Thus, K_e varies from 1 for a head-on collision to 0 in the limit of the iceberg just making glancing contact with the structure.

Added mass

The added mass of an iceberg at impact, C_m, is determined by solving the boundary value problem corresponding to an iceberg undergoing small amplitude oscillations in otherwise still water. A description of the calculation procedure has

Fig. 3. Sketch of force–displacement relations showing energy dissipated through ice crushing displacement x_c and structural damage displacement x_d.

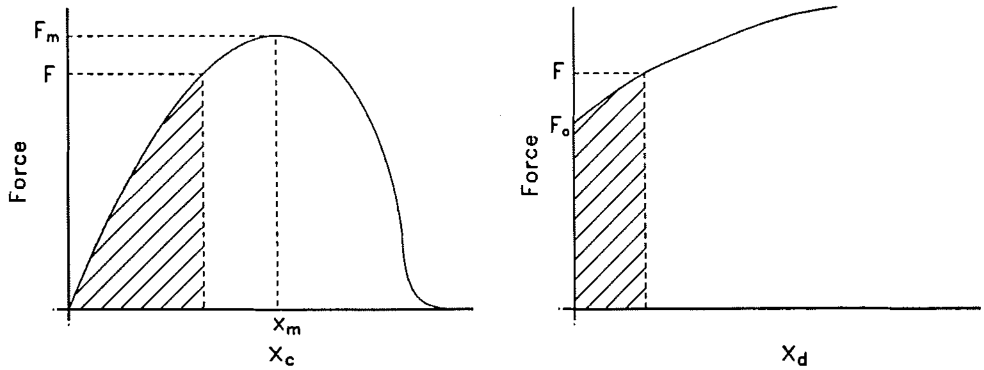

been given by Isaacson and Cheung (1988*a*, 1988*b*). In general, the added mass is frequency dependent, although it is customary to use a single value (usually the zero frequency value) when treating the iceberg impact problem. The added mass of the iceberg depends on the submerged geometry, the water depth, and the submerged geometry of any neighbouring structure (and thus it is a function of the iceberg distance from any such structure). The zero-frequency added mass is estimated here for a range of iceberg parameters, both in open water and when in contact with the structure. However, for the range of iceberg sizes of interest, the added mass is not strongly influenced by the proximity to the structure. Once more, a simple expression has been derived from numerical results obtained over a range of conditions:

$$[21] \quad C_m = 0.0883\left(\frac{D}{d}\right)\left(\frac{h}{d}\right) + 0.6386\left(\frac{h}{d}\right) - 0.0998\left(\frac{D}{d}\right) + 0.2229$$

Force due to iceberg collision and waves

Attention is now given to a consideration of an iceberg collision in the presence of waves. The preceding descriptions of iceberg shape and size, crushing pressure, and added mass continue to apply. However, the maximum force on the structure is altered, partly because the impact velocity is changed, partly because of the wave force which now acts on the structure, and partly because the wave force on the iceberg influences the iceberg force on the structure. Furthermore, the description of wave parameters must now reflect the sea state at the moment of collision, so that more commonly occurring wave conditions should be accounted for. These aspects are now considered further.

Wave parameters

For convenience, the description of more commonly occurring wave conditions is assumed to derive from measurements based on a specified recording interval τ, taken here as 6 h. The corresponding probability distribution of the wave period T can be obtained from the distribution of the annual maximum period, given in [4], by raising the latter to the power of $1/N$, where N is the number of such intervals per year. ($N = 365 \times 24/\tau$, where τ is in hours, so that for a recording interval of 6 h, $N = 1460$.) However, this approach produces unrealistic results due to the unreliability of [4] at high probability exceedence levels corresponding to $T < 15$ s, particularly in that [4] underpredicts the probability of relatively frequent low period (and height) wave events. To correct for this, the lower tail of [4] (for $T < 15$ s) has been modified so as to be more realistic for relatively frequent wave events. The modified distribution was taken as

$$[22] \quad p(T) = \begin{cases} \exp\left[-\exp(-(0.45542 \times 10^{-3} T^{3.6046} - 9.0))\right] & \text{for } T < 15 \\ \exp\left[-\exp(-1.8991(T - 15.5777))\right] & \text{for } T \geq 15 \end{cases}$$

The above distribution is identical to [4] for $T \geq 15$ s, and meets continuity conditions with respect to its value and slope at $T = 15$ s. Also, the corresponding distribution of commonly occurring waves (obtained by raising [22] to the power of $1/N$) provides a small but finite probability of encountering calm conditions ($T \rightarrow 0$ s) for part of the year. The value of 9.0 in [22] was selected in a somewhat arbitrary manner so as to result in a mean wave period of about $T = 10$ s for commonly occurring waves, and a probability of 0.5% of encountering calm water during any single measurement. The sensitivity of the results to the choice of this value was investigated, and was found to be negligible for values in the range 8.5 to 10.0, which is considered to be a maximum probable range (for example, for 8.5, the probability of encountering calm water is already 3.5%).

Impact velocity

Although data for the open water drift velocity of icebergs are generally available, the iceberg's velocity may differ from such data when storm waves are present and when it approaches the structure. First, the waves give rise to a wave drift force which causes an increase in the iceberg velocity. This is likely not adequately accounted for in iceberg drift data, since such data generally pertain to commonly occurring wave conditions, whereas design waves with a return period of the order of 100 years are of interest here. Second, since the wave drift force and iceberg added mass vary with distance from the structure, the iceberg velocity may be further modified through its equations of motion as it approaches the structure. Overall, it is expected that the impact velocity V depends on the current velocity U, the iceberg dimensions (characterized by its waterline diameter D and draft h), and the prevailing wave conditions characterized by H_s or T.

A simple formulation for the iceberg impact velocity V may be developed by taking V to be proportional to the iceberg drift velocity in open water, denoted V_o, and adopting a suitable expression for the latter. Following Isaacson (1988), an expression for V_o may be developed by equating the wave drift force to the current drag, taking the wave drift force coefficient to be proportional to D/L (see Isaacson 1988), where L is the wavelength, and using [5] to relate wave height and wave period. The above approach gives rise to the following expression for the impact velocity V:

$$[23] \quad V = U + \alpha g T\sqrt{\frac{D}{h}}$$

where α is a constant and g is the gravitational constant.

The value of the constant α has been estimated by examining previous results and data for the open water velocity V_o (e.g., Lever and Sen 1987) in the context of [23]; and using a numerical model to relate the impact velocity V to the open water velocity V_o. Thus, a wave diffraction–radiation analysis has been carried out for a series of conditions corresponding to the iceberg approaching the structure, using an extension to the computer program WELSAS. This provides solutions to the two-body diffraction–radiation problem of a floating iceberg approaching a fixed structure, as well as to the iceberg's equations of motion, and has been described by Isaacson (1987). For each such condition, the submerged surfaces of the structure and iceberg are discretized into a number of quadrilateral facets for a boundary element method analysis, in order to obtain the trajectory of the iceberg and the impact velocity V.

Overall, the foregoing procedure has indicated that [23] should be suitable for the conditions of interest here with the constant in [23], α, taken as 0.003. It turns out that, for extreme storm conditions, [23] predicts impact velocities which may be more than twice that of the current velocity.

Maximum force

The calculation of the maximum force F_M on the structure requires a search for the maximum combination of the iceberg force on the structure, $F(x)$, and the wave force on the structure, $F_w^{(s)}$ (see Fig. 4), from the instant of initial impact, $t = 0$, until the iceberg is stopped, $t = t_o$, bearing in mind that at maximum penetration the wave force $F_w^{(s)}$ may not be at its peak. That is,

$$[24] \quad F_M = \max\{F(x) + F_w^{(s)}\} \qquad \text{for } 0 \le t \le t_o$$

In the presence of waves, the iceberg force on the structure, $F(x)$, is itself influenced in part by the wave force on the iceberg, $F_w^{(i)}$, and thus the calculation of $F(x)$ is carried out by a direct integration of the equation of motion of the iceberg, rather than by a simple energy balance as in [18]. Thus, Fig. 4 shows the iceberg of mass M under the force $F(x)$, due to ice crushing, and the wave force $F_w^{(i)}$, and the dynamic equilibrium of the iceberg gives rise to the following equation of motion for the iceberg:

$$[25] \quad M(1 + C_m)\ddot{x} = -F(x) + F_w^{(i)}$$

Fig. 4. Sketch of dynamic equilibrium of the iceberg and wave and iceberg forces on the structure.

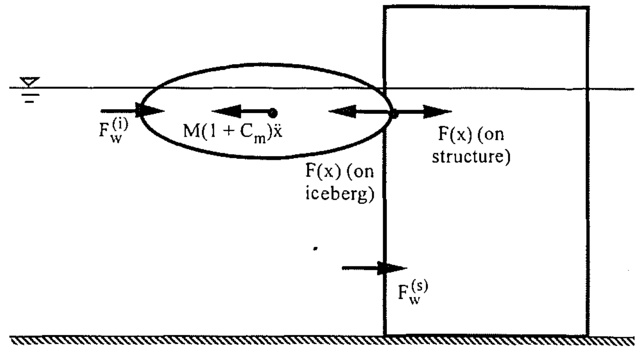

with initial conditions $x = 0$ and $\dot{x} = V$ at $t = 0$, and an overdot denoting a derivative with respect to time. The force $F_w^{(i)}$ of the waves on the iceberg is expressed as

$$[26] \quad F_w^{(i)} = F_w^{*(i)}\cos(\omega t - \varepsilon)$$

where $\omega = 2\pi/T$ is the angular frequency, and the phase angle ε varies between 0 and 2π.

The wave force amplitude $F_w^{*(i)}$ has been calculated for a range of iceberg and wave parameters using an extension to the computer program WELSAS. The combined submerged surface of the iceberg in contact with the structure is discretized into a number of quadrilateral facets, and the magnitudes and phases of forces acting on the iceberg and structure are each computed by suitable integrations of the hydrodynamic pressure acting on the combined configuration. Since this approach in effect treats the iceberg and structure as a single contiguous body, rather than as two bodies in close proximity, no particular numerical difficulties are encountered. The numerical results are expressed as follows:

$$[27] \quad F_w^{*(i)} = 0.0172\, h\frac{D^2}{T^2} H C_F^{(i)}$$

where $F_w^{*(i)}$ is in MN, H (m) is the wave height, and the force coefficient $C_F^{(i)}$ is given by

$$[28] \quad C_F^{(i)} = \left[2.25 - 3.0\left(\frac{D}{\lambda}\right) + \left(\frac{D}{\lambda}\right)^2\right] \times [2.5255 \times 10^{-1} + 4.0111 \times 10^{-3} D - 5.6944 \times 10^{-6} D^2]$$

The wavelength λ may be obtained in terms of the wave period T on the basis of the linear dispersion relationship. First, the relative depth parameter kd, where k ($= 2\pi/\lambda$) is the wave number, is obtained by an iterative solution of the following equation:

$$[29] \quad kd\tanh(kd) = 4\pi^2\left(\frac{d}{gT^2}\right)$$

where g is the gravitational constant ($= 9.81$ m/s^2). The wavelength λ is then obtained directly from the wave number (since, by definition, $\lambda = 2\pi/k$).

As already indicated in Fig. 2, the iceberg force on the structure, $F(x)$, is a nonlinear function of x. However, the iceberg will be stopped at values of x for which the function $F(x)$ can be linearized as follows:

$$[30] \quad F(x) = Kx$$

where K is the initial slope of the force–penetration relationship. With this linearization of the force $F(x)$, the equation of motion, [25], can readily be integrated in closed form. Of particular interest is the time t_o at which the velocity $\dot{x}$ first vanishes (iceberg stopped), and the corresponding maximum penetration. The maximum iceberg force on the structure is obtained from the force–penetration relationship up to the point of maximum penetration.

The force due to waves acting on the structure itself is also required (see Fig. 4). This force must reflect, however, the presence of the iceberg. This force, $F_w^{(s)}$, is calculated as described earlier by treating the wave diffraction problem for the combined submerged surface of the iceberg in contact with the structure, with only a pressure integration over the structure surface used to provide the wave force on the structure. The corresponding numerical results are expressed as

$$[31] \quad F_w^{(s)} = 0.01012a^2\frac{H}{T^2}\lambda C_F^{(s)}\cos(\omega t - \varepsilon + \phi)$$

where $F_w^{(s)}$ is in MN, ϕ is the phase angle between the wave force on the iceberg and the corresponding wave force on the structure. The force coefficient $C_F^{(s)}$ is obtained in the form:

$$[32] \quad C_F^{(s)} = a_1 + a_2\left(\frac{2a}{\lambda}\right) + a_3\left(\frac{2a}{\lambda}\right)^2$$

where the coefficients a_1, a_2, and a_3 are functions of the draft h and the waterline diameter D:

$$[33a] \quad a_1 = (1.4756 + 3.8331 \times 10^{-2}h - 3.8052 \times 10^{-4}h^2) \times (1.9395 - 9.2436 \times 10^{-3}D + 1.8093 \times 10^{-5}D^2)$$

$$[33b] \quad a_2 = (-3.6095 - 0.9351 \times 10^{-1}h + 1.0916 \times 10^{-3}h^2) \times (1.7296 - 6.7278 \times 10^{-3}D + 1.0832 \times 10^{-5}D^2)$$

$$[33c] \quad a_3 = (2.1619 + 0.7938 \times 10^{-1}h - 1.0134 \times 10^{-3}h^2) \times (1.6132 - 4.7543 \times 10^{-3}D + 2.6709 \times 10^{-6}D^2)$$

The phase angle ϕ between the forces $F_w^{(i)}$ and $F_w^{(s)}$ is also required, and has been calculated as

$$[34] \quad \phi = a_4 + a_5\left(\frac{2a}{\lambda}\right)$$

where the coefficients a_4 and a_5 depend on the iceberg's waterline diameter D:

$$[35a] \quad a_4 = -248.87 - 1.7507D + 4.0953 \times 10^{-3}D^2$$

$$[35b] \quad a_5 = -320.31 + 9.523D - 1.6477 \times 10^{-2}D^2$$

Given the oscillatory character of the wave force on the iceberg, $F_w^{(i)}$, this force sometimes pushes the ice mass forwards and sometimes backwards. The phase angle ε, which controls the effect of this force at time $t = 0$ (i.e., at the beginning of the collision), therefore has a substantial importance in the calculation of the exceedence probability. The FORM calculations are done conditional on specific values of the phase angle ε, with the total exceedence probability then calculated by integration over all phase angles from 0 to 2π. The integration is facilitated by the simple probability density function of the uniform distribution for ε, using a Gaussian scheme with five integration points.

Modifications to the probability distributions for *U* and *L*

The statistics for U and L correspond to all icebergs in open water. However, these differ from the corresponding statistics for impacting icebergs, since an iceberg's speed and size influence its probability of collision with the structure. Sanderson (1988) has investigated this difference (see also Maes and Jordaan 1984) and has shown that the speed and size probability distributions for colliding icebergs can be obtained as modifications of the corresponding distributions of all icebergs in open water. An application of Bayes' theorem enables the expressions of the modified probability density functions for U and L to be given as follows:

$$[36] \quad f^*(U) = f(U)\left(\frac{U}{\bar{U}}\right)$$

$$[37] \quad f^*(L) = f(L)\left(\frac{a + L}{a + \bar{L}}\right)$$

where $f(U)$ and $f(L)$ are the corresponding open water probability density functions, and $\bar{U}$ and $\bar{L}$ are the corresponding mean values. It is seen that [36] and [37] skew the original distributions so as to increase the chances of collision of bigger and faster icebergs.

Comparison between FORM results and Monte Carlo simulations

It is useful to compare the accuracy of the FORM results against those of straightforward Monte Carlo simulations. Figure 5 shows the exceedence probabilities associated with different load levels F, obtained using FORM and Monte Carlo simulation, when only iceberg collisions are considered (waves absent) and neither structural damage nor the modifications of [20], [36], and [37] are included. For this comparison, $p_o = 2$ MPa and $V_p = 0.5$. The model error variable R_{n1} is assumed normally distributed, with a mean of 1 and a standard deviation of 0.15. At 500 MN, the design point includes a velocity $V = 0.55$ m/s and an iceberg of dimensions $L = 143.0$ m and $h = 67.9$ m. From higher to lower, the sensitivity of the results to variable uncertainty is ordered as follows: V, L, h, ice crushing variable R_{n4}, and model uncertainty R_{n1}. It is apparent from Fig. 5 that FORM produces excellent results in comparison to simulation. FORM also results in very efficient and fast calculations (0.5 s per load level using a 486 PC at 33 MHz).

Figure 6 shows a comparison, at low exceedence probabilities, of maximum forces with or without structural damage. It appears that structural damage introduces only small changes, reducing the probability for a given load level. This

Fig. 5. Comparison between FORM and Monte Carlo simulations for iceberg impact force.

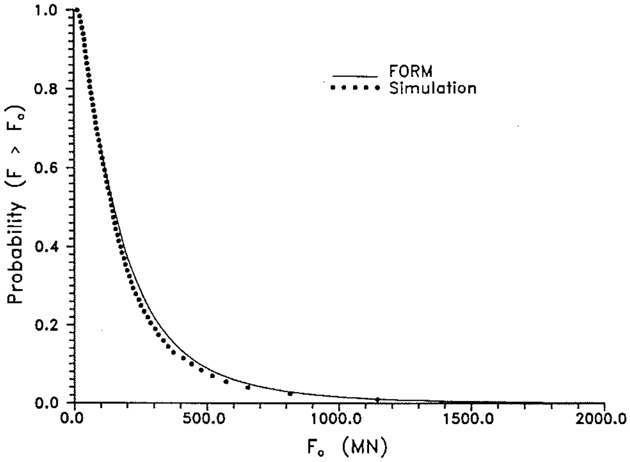

Fig. 6. Influence of structural damage on iceberg collision force cumulative distribution function.

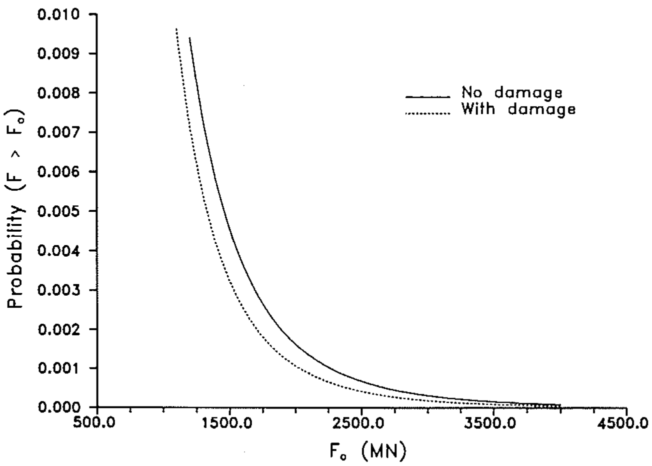

implies that the cumulative distribution function of maximum load is mostly controlled by energy dissipation through ice crushing. Using a Poisson arrival process with a mean rate of 0.08 collisions/year, the 100-year iceberg corresponds to an event exceedence probability of 0.126. On this basis, the 100-year iceberg force is estimated at 381 MN, a level that is not influenced by consideration of damage, given the threshold force F_0 = 610 MN (see [19]).

Finally, Fig. 7 shows the substantial effect of the corrections arising from [36] and [37]. The shift to faster and larger icebergs implies large changes to the cumulative distribution function, emphasizing the importance of correctly modelling collision probability. In this case, the corresponding 100-year iceberg force becomes 717 MN.

Results

Table 1 shows a summary of the statistical parameters that have been used for the various specified random variables, except that the parameters for the iceberg draft h are determined by those of L. In order to verify the load combination factors specified in the Code, it is necessary to use these

Fig. 7. Influence of shifted distributions for U and L on iceberg collision force cumulative distribution function.

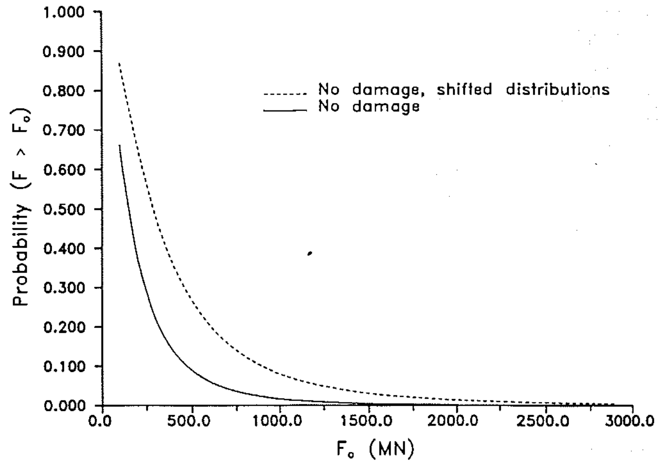

Table 1. Summary of random variables and their statistics.

Variable	Distribution	Characteristics
Iceberg length, L	Gamma	μ = 121.60 m σ = 56.70 m
Iceberg draft, h	Beta	μ = 61.35 m σ = 12.38 m min = 0.00 m max = 80.00 m
Current velocity, U	Lognormal	μ = 0.32 m/s σ = 0.27 m/s
Wave period, T (annual maximum)	Extreme type I	μ = 15.89 s σ = 0.67 s
R_{n1}, associated with model uncertainty	Normal	μ = 1.0 σ = (input)
R_{n2}, sand friction angle	Normal	μ = 35.0° σ = 7.0°
R_{n3}, associated with uncertainty in structure weight W	Normal	μ = 1.0 σ = (input)
R_{n4}, associated with ice-crushing pressure p	Normal	μ = 0.0 σ = 1.0
R_{n5}, associated with slope of load − damage deformation relationship	Lognormal	μ = 1.0 σ = (input)
R_{n6}, associated with collision eccentricity	Uniform	min = 0.0 max = 1.0
R_{n7}, associated with Rayleigh distribution for wave height H	Uniform	min = 0.0 max = 1.0

Table 2. Maximum wave force F_M for annual exceedence probabilities of 10^{-2} and 10^{-4}.

Annual exceedence probability	Maximum wave force F_M (MN)
10^{-2}	1496
10^{-4}	2376

Table 3. Maximum iceberg force F_M for annual exceedence probabilities of 10^{-2} and 10^{-4} and various values of iceberg arrival rate μ and ice-crushing pressure threshold p_o.

Annual exceedence probability	Iceberg arrival rate μ (collisions/year)	U, L distribution modification	Maximum iceberg force F_M (MN)		
			p_o = 2 MPa	p_o = 4 MPa	p_o = 6 MPa
10^{-2}	0.04	No	248	351	431
	0.08	No	381	537	657
	0.20	No	587	830	1017
	1.00	No	1061	1503	1843
	0.08	Yes	717	1015	1245
10^{-4}	0.04	No	1605	2276	2792
	0.08	No	1932	2740	3360
	0.20	No	2425	3442	4224
	1.00	No	3484	4952	6080
	0.08	Yes	3588	5106	6270

parameters to obtain the wave loads for an annual exceedence level of 10^{-2} and both the iceberg alone and the iceberg plus waves loads at an annual exceedence level of 10^{-4}.

The program WLOAD was first run to obtain the forces for waves alone at annual exceedence probabilities of 10^{-2} and 10^{-4} and the corresponding results are shown in Table 2. Although the load at the latter probability level is not needed for the combination event, it is included for completeness. It turns out that the force of 1496 MN shown for an annual exceedence probability of 10^{-2} is associated with an individual wave height H of 19.2 m occurring during a sea state with a wave period T of 16.4 s, and a significant wave height H_s of 13.7 m. This sea state itself has a return period of about 5.5 years. This emphasizes that the traditional approach of selecting a sea state (significant wave height) with the required exceedence probability, and then selecting the expected maximum individual wave height within that sea state, may be unduly conservative.

The program ICELOAD was run to obtain the forces for iceberg collision alone at exceedence probabilities of 10^{-2} and 10^{-4} and the corresponding results are shown in Table 3. Although the first is not required for the combination event, it is included here in order to provide data for prospective comparisons with other work in this field and for calculations regarding serviceability and section strength limit strengths. Table 3 indicates the influence of the annual exceedence probability, the iceberg arrival rate μ, the modifications to the U and L distributions as described in [36] and [37], and the ice crushing pressure threshold p_o. The table indicates that the iceberg collision forces are strongly dependent on all four of these factors. In particular, it is apparent that the modifications to the distributions for U and L have a marked effect on the collision forces, and must be taken into account when the goal is to estimate the level of those forces for design.

Finally, the program ICEWLOAD was run to obtain the total force on the structure as a result of an iceberg collision in the presence of waves, and the corresponding results are shown in Table 4. The annual exceedence probability was set at 10^{-4}, as required by the Code. Once more, the table indicates the influence of the iceberg arrival rate μ, the modifications to the U and L distributions as described in [36] and [37], and the ice crushing pressure threshold p_o. Once more, as in the case of an iceberg collision alone, all these factors have a marked influence on the maximum combined load. The results given in Table 4 were all obtained for a wave measurement recording interval τ of 6 h, corresponding to N = 1460. In fact, the use of different values of recording interval τ was examined, and τ was found not to affect the results noticeably.

The above results can be extended to determine the structural weight W that would result in an annual risk level of 10^{-4} if a deterministic sand friction angle is specified. For example, for a friction angle of 35°, this weight would be $W = F/\tan 35° = 1.428F$, where F denotes a suitable force entry in Table 4.

Load combination factors

The load combination factor γ is used in the CSA code to determine a design value for the load due to a companion frequent environmental process (waves) acting in combination with a rare environmental event (iceberg collision). The load combination factor γ is defined in the Code by

$$[38] \quad E = E_r + \gamma E_f$$

where E is the combined load with an annual exceedence probability of 10^{-4}, E_r is the iceberg alone load with an annual exceedence probability of 10^{-4}, and E_f is the wave load with an annual exceedence probability of 10^{-2}. Thus the factor γ aims to achieve a combined wave–iceberg load with an annual risk of 10^{-4}, just as the iceberg alone load would be required to the same annual risk of 10^{-4} if waves were not present.

The CSA code recommends γ = 0.8 for stochastically dependent events or processes and γ = 0.4 for stochastically independent events or processes, and that iceberg impact and waves should be considered stochastically independent (i.e., γ = 0.4).

Values of γ can be calculated from the results given in Tables 2–4, and are shown in Table 5. Although the actual loads are substantially influenced by the iceberg arrival rate, the ice crushing pressure threshold p_o, and the application of the distribution modifications [36] and [37], the results in

Table 4. Maximum combined wave–iceberg force F_M for an annual exceedence probability of 10^{-4} and various values of iceberg arrival rate μ and ice-crushing pressure threshold p_o.

Iceberg arrival rate μ (collisions/year)	U, L distribution modification	Maximum combined wave–iceberg load F_M (MN)		
		p_o = 2 MPa	p_o = 4 MPa	p_o = 6 MPa
0.04	No	2305	3120	3797
0.08	No	2592	3604	4394
0.20	No	3088	4331	5287
1.00	No	4175	5880	7189
0.08	Yes	4220	5952	7281

Table 5. Load combination factor γ for an annual exceedence probability of 10^{-4} and various values of iceberg arrival rate μ and ice-crushing pressure threshold p_o.

Iceberg arrival rate μ (collisions/year)	Distribution modification	Load combination factor γ		
		p_o = 2 MPa	p_o = 4 MPa	p_o = 6 MPa
0.04	No	0.47	0.56	0.67
0.08	No	0.44	0.58	0.69
0.20	No	0.44	0.59	0.71
1.00	No	0.46	0.62	0.74
0.08	Yes	0.42	0.57	0.68

Table 5 suggest that the load combination factor itself is much more stable, and essentially only exhibits an effect of p_o. Since the iceberg collision force is interrelated with the effect of the waves, the combined event should be classified as dependent. However, the corresponding load combination factor of 0.80 is on the conservative side, with the actual value depending on the assumed level of p_o. The value of 0.40 given in the Code is reasonably consistent with a low value of p_o = 2 MPa, but γ should be increased to approximately 0.60 and 0.70 for p_o = 4 MPa and 6 MPa respectively.

Conclusions

The analysis of loads due to an iceberg collision during a storm is presented. Mechanics models have been developed to provide forces on an offshore structure due to (*i*) waves alone, (*ii*) an iceberg alone, and (*iii*) the combination of waves with an iceberg. These have been combined with a reliability model in order to develop forces corresponding to specified risk levels.

The maximum combined load on the structure is associated with a number of factors. There is a significant increase of iceberg impact velocity due to the presence of waves. The presence of an iceberg considerably influences the wave field around the structure, and thus influences the wave force on the structure. Likewise, the presence of the structure influences the wave force on the iceberg, which in turn influences the iceberg force on the structure. The maximum combined force on the structure occurs at some instant between initial impact and the iceberg stopping, and must be determined.

One objective of this study has been to examine and recommend suitable load combination factors for combined iceberg–wave loads on large offshore structures. At present, the CSA code recommends that iceberg impact and waves should be considered stochastically independent, with a load combination factor γ of 0.4. The present study suggests that iceberg impact and waves should instead be considered stochastically dependent, but that for the particular structure and water depth considered, the value of γ should be dependent on the ice crushing pressure threshold p_o. Thus, further experimental research relating to ice-crushing behaviour for large contact areas is required. On the other hand, the load combination factor of about 0.8 for dependent events can be safely applied for a range of p_o, iceberg arrival rates, and whether or not the distributions for U and L are modified for colliding icebergs. Although not shown, this work also considered the load combination factors corresponding to an annual risk level of 10^{-5}, with wave loads at 10^{-2} and iceberg loads at 10^{-5}, with similar results.

References

Bass, D., Gaskill, H., and Riggs, N. 1985. Analysis of iceberg impacts with gravity base structures at Hibernia. Proceedings of the 4th International Conference on Offshore Mechanics and Arctic Engineering, Dallas, Tex., Vol. II, pp. 255–259.

Bea, R.G. 1992. Evaluation of uncertainties in loading on offshore structures due to extreme environmental conditions. Proceedings of the 11th International Offshore Mechanics and Arctic Engineering Symposium, Calgary, Alta., Vol. II, pp. 367–376.

Blanchet, D. 1990. Ice design criteria for wide arctic structures. Canadian Geotechnical Journal, **27**(6): 701–725.

Canadian Standards Association. 1992. General requirements, design criteria, environment and loads. (Forming part of the code for the design, construction, and installation of fixed offshore structures.) CAN/CSA-S471-92, Canadian Standards Association, Rexdale, Ont.

Cammaert, A.B., and Muggeridge, D.B. 1988. Ice interaction with offshore structures. Van Nostrand Reinhold, New York.

Det Norske Veritas. 1988. Probabilistic framework for ice loads on fixed marine structures. Calgary, Alta. Report to Department of Public Works, Ottawa, Ont., Vol. 1.

El-Tahan, H., Venkatesh, S., and El-Tahan, M. 1986. Evaluation of a model for predicting the drift of iceberg ensembles. Proceedings of the 5th International Offshore Mechanics and Arctic Engineering Symposium, Tokyo, Japan, Vol. IV, pp. 418–425.

Foschi, R.O., Folz, B., and Yao, F. 1990. RELAN: User's manual. Department of Civil Engineering, The University of British Columbia, Vancouver, B.C.

Fuglem, M.K., Duthinh, D., Lever, J.H., and Jordaan, I. 1991. Probabilistic determination of iceberg collision design loads for floating production vessels. Proceedings of the IUTAM–IAHR Symposium on Ice–Structure Interaction, St. John's, Nfld., Springer-Verlag, New York, pp. 459–482.

Fuglem, M., Jordaan, I., Crocker, G., Cammaert, G., and Berry, B. 1996. Environmental factors in iceberg collision risks for floating systems. Cold Regions Science and Technology, in press.

Isaacson, M. 1987. Ice mass motions near an offshore structure. Journal of Offshore Mechanics and Arctic Engineering, **109**(2): 206–210.

Isaacson, M. 1988. Influence of wave drift force on ice mass motions. Proceedings of the 7th International Conference on Offshore Mechanics and Arctic Engineering, Houston, Tex., Vol. II, pp. 125–130.

Isaacson, M., and Cheung, K.F. 1988*a*. Hydrodynamics of an ice mass near an offshore structure. Journal of Waterway, Ports, Coastal and Ocean Engineering, **114**(4): 487–502.

Isaacson, M., and Cheung, K.F. 1988*b*. Influence of added mass on ice impacts. Canadian Journal of Civil Engineering, **15**(4): 698–708.

Isaacson, M., and Dello-Stritto, F.J. 1986. Motion of an ice mass near a large offshore structure. Proceedings of the 18th Offshore Technology Conference, Houston, Tex., Paper No. OTC 5085, Vol. 1, pp. 21–27.

Lever, J.H., and Sen, D. 1987. A method to upgrade iceberg velocity statistics to include wave-induced motion. Journal of Offshore Mechanics and Arctic Engineering, **109**(3): 278–286.

Lever, J.H., Attwood, D., and Sen, D. 1988. Factors affecting the predictions of wave-induced iceberg motion. Cold Regions Science and Technology, **15**: 177–190.

Lever, J.H., Colbourne, B., and Mak, L. 1990. Model study of the wave-driven impact of bergy bits with a semi-submersible platform. Journal of Offshore Mechanics and Arctic Engineering, **112**(4): 313–322.

Lindberg, K., and Anderson, L. 1987. Ice impacts on semi-submersibles. Proceedings of the 6th International Conference on Offshore Mechanics and Arctic Engineering, Houston, Tex., Vol. IV, pp. 313–320.

Maes, M.A. 1986. Calibration of partial factors in the new CSA Code for fixed offshore production structures. Environmental Protection Branch, Canada Oil and Gas Lands Administration, Energy Mines and Resources, Ottawa, Ont., Technical Report No. 9.

Maes, M.A., and Jordaan, I. 1984. Probabilistic analysis of iceberg loads on offshore structures. Proceedings of the International Association for Hydraulic Research Ice Symposium, Hamburg, Germany, pp. 175–188.

Neu, H.J.A. 1982. 11-year deep water wave climate of Canada Atlantic waters. Canadian Technical Report of Hydrography and Ocean Sciences, Ottawa, Ont., No. 13.

Salvalaggio, M.A., and Rojansky, M. 1986. The importance of wave-driven icebergs impacting an offshore structure. Proceedings of the 18th Offshore Technology Conference, Houston, Tex., Paper No. OTC 5086, Vol. 1, pp. 29–38.

Sanderson, T.J.O. 1988. Ice mechanics and risks to offshore structures. Graham and Trotman, London, United Kingdom.

Sarpkaya, T., and Isaacson, M. 1981. Mechanics of wave forces on offshore structures. Van Nostrand Reinhold, New York.

List of symbols

A	iceberg contact area with structure
a	structure radius (see Fig. 1)
B	iceberg vertical (minor) semiaxis (see Fig. 1)
C_F	force coefficient
C_m	added mass coefficient
D	iceberg waterline diameter (see Fig. 1)
d	still water depth
E	combined load with an annual exceedence of 10^{-5}
E_f	wave load with an annual exceedence of 10^{-2}
E_r	iceberg alone load with an annual exceedence of 10^{-4}
F	force
$F(x)$	iceberg force on structure
F_M	maximum force on structure
F_o	minimum force for structural damage (see [19])
$F_w^{(i)}$	wave force on iceberg
$F_w^{(s)}$	wave force on structure
G	performance function (see [1] and [2])
g	gravitational constant
H	wave height
H_s	significant wave height
h	iceberg draft (see Fig. 1)
K	initial slope of force–penetration curve
k	wave number ($= 2\pi/\lambda$)
K_e	eccentricity reduction factor
L	characteristic iceberg length
M	iceberg mass
N	number of wave measurements per year
p	iceberg crushing pressure; cumulative probability
p_a	annual risk
p_e	conditional exceedence probability
p_o	ice crushing pressure threshold (see [14])
R	iceberg horizontal (major) semiaxis (see Fig. 1)
R_n	random variable (see Table 1)
T	wave period
T_R	return period
t	time
t_o	time at which iceberg is stopped
U	current magnitude
V	iceberg impact velocity
x	iceberg penetration (see Fig. 3)
x_c	iceberg penetration due to crushing
x_d	iceberg penetration due to structural damage
α	constant in impact velocity formulation (see [23])
γ	load combination factor (see [38])
ε	phase angle (see [26])
λ	wavelength
μ	mean; mean rate of annual occurrence; iceberg arrival rate
σ	standard deviation
τ	recording interval of wave measurements
ϕ	phase angle between $F_w^{(i)}$ and $F_w^{(s)}$ (see [31])
ω	wave angular frequency ($= 2\pi/T$)